

Classification

Physics Abstracts

61.30B — 64.70M — 64.60F

Critical behaviour of a lattice model of the nematic to smectic-A transition

C. Dasgupta

School of Physics and Astronomy, University of Minnesota, Minneapolis, MN 55455, U.S.A.

(Reçu le 15 octobre 1986, accepté le 19 décembre 1986)

Résumé. — On présente une version sur réseau du modèle de de Gennes pour la transition nématique-smectique A ; son comportement critique est étudié par des simulations suivant la méthode de Monte Carlo. Ces simulations reproduisent qualitativement certains comportements observés dans les expériences. Le modèle présente une transition de phase continue dont l'exposant α pour la chaleur spécifique est proche de zéro. Les fonctions de corrélation du paramètre d'ordre ont un comportement critique anisotrope à l'approche de la transition du côté nématique. D'autre part, le comportement des fonctions de corrélation dans la jauge supraconductrice implique un point critique isotrope aussi bien pour les grandes que pour les petites valeurs de la constante élastique qui décrit des déformations en éventail. Le comportement observé pour les constantes élastiques de flexion et de torsion est cohérent avec cette conclusion. La dépendance en jauge des fonctions de corrélation semble être bien décrite par l'hypothèse de découplage proposée par Lubensky *et al.*

Abstract. — The critical behaviour of a lattice version of the de Gennes model of the nematic to smectic-A transition is studied by Monte Carlo simulations. Several features observed in experiments are qualitatively reproduced in the simulations. The model exhibits a continuous phase transition with the specific heat exponent α close to zero. The order-parameter correlation functions show anisotropic critical behaviour as the transition is approached from the nematic side. On the other hand, the observed behaviour of the correlation functions in the superconducting gauge strongly indicates an isotropic critical point for both small and large values of the splay elastic constant. The observed behaviour of the twist and bend elastic constants is consistent with this conclusion. The gauge-dependence of the correlation functions appears to be well-described by the decoupling approximation proposed by Lubensky and co-workers.

1. Introduction.

Since the early 1970's, the nematic to smectic-A (NA) transition in liquid crystals has been the subject of many experimental [1] and theoretical [2] studies. In spite of these efforts, this transition remains one of the most intriguing and least understood problems in the field of equilibrium critical phenomena. Most of the theoretical studies of this phase transition have been based on a phenomenological model proposed by de Gennes [3] in 1972. In this model, the smectic order is described by a complex scalar field Ψ and a two-component real vector field $\delta\mathbf{n}$ describes small fluctuations of the nematic director about its equilibrium orientation. The fields Ψ and $\delta\mathbf{n}$ are coupled in a way that makes the free-energy functional invariant under a small global rotation [4]. The de Gennes free-energy functional is formally very similar to the Ginzburg-

Landau free-energy functional for superconductors, with Ψ playing the role of the superconducting order-parameter field, and $\delta\mathbf{n}$ playing the role of the vector potential. This analogy with the superconducting transition has been used extensively [5-7] in theoretical studies of the NA transition. There remain, however, several important differences between the superconductor and the smectic-A liquid crystal. These differences include the absence of true long-range smectic order in three dimensions [8, 9], the inherently anisotropic nature of the smectic phase and the presence of the splay elastic term [10] in the de Gennes free-energy functional. An understanding of whether these differences are relevant in the critical region is necessary before one can draw any conclusion about the nature of the NA transition from the superconducting analogy. Recently, there have been attempts [11-13] to describe the NA transition in three dimensions as an unbinding of

dislocation loops. The model of interacting dislocation loops considered in these studies can be derived [14-15] from the de Gennes free energy. The dislocation-melting theories are, therefore, completely equivalent to a description within the framework of the de Gennes model.

At the present time, there exist no theoretical consensus about the critical behaviour of the de Gennes model. Many years ago, Halperin, Lubensky and Ma [5] used a fluctuation-corrected mean-field theory and a renormalization-group analysis near four dimensions to argue that both the superconducting and the NA transition [6] should be weakly first-order in nature. Experimentally, however, the NA transition often appears to be continuous [1]. A possible explanation of this contradiction between theory and experiments has been provided by more recent analytic [16] and numerical [16, 17] studies of lattice models of superconductivity. These studies provide compelling evidence indicating that the three-dimensional type-II superconductor exhibits a continuous phase transition that belongs to the so-called « inverted XY » universality class. This universality class represents second order phase transitions with critical exponents identical to those in the three-dimensional XY model, but distinguished by the fact that the temperature asymmetries of the specific heat and other singular quantities in the critical region are inverted [16] relative to the XY transition. A recent renormalization-group study [13] of a field-theoretic version of the dislocation loop model of the NA transition indicates that this transition should also exhibit inverted XY behaviour, at least for small values of the splay elastic constant K_1 . However, there exist other theoretical arguments [11, 12] based on the dislocation melting mechanism which predict anisotropic scaling [7] in the critical region, with the correlation length exponents ν_{\parallel} and ν_{\perp} for fluctuations parallel and perpendicular to the direction of smectic ordering having the ratio 2:1. The current theoretical view of the nature of the phase transition in the de Gennes model has been summarized in the review article of Lubensky [2]. According to this account, the three-dimensional model with a finite splay elastic constant allows two asymptotic possibilities. These are : a) an isotropic ($\nu_{\parallel} = \nu_{\perp}$) critical point in the inverted XY universality class, and b) a critical point described by anisotropic scaling with $\nu_{\parallel} = 2 \nu_{\perp}$. For the isotropic case, the critical exponents have the same values as those for the λ -transition of liquid helium. There is as yet no theoretical prediction about the values of the critical exponents for the anisotropic universality class.

For a determination of which one of these two possibilities is realized in nature, it is necessary to understand how the universality class of the transition manifests itself in the critical behaviour of

experimentally measurable quantities. This requires an understanding of the « gauge-dependence » of the quantities of interest. The original, physical variables Ψ and $\delta \mathbf{n}$ appearing in the de Gennes model define the so-called liquid crystal (LC) gauge. All experimental observations are restricted to this gauge. Divergent fluctuations in the phase of the order parameter in this gauge lead to the well-known destruction [8, 9] of true long-range smectic order in three dimensions. It is, however, possible to cast the description in terms of a different set of variables which are related to Ψ and $\delta \mathbf{n}$ through a gauge transformation [2, 6, 7]. In particular, it is possible [6] to define a new gauge (the so-called superconducting (SC) gauge) in which phase fluctuations are not divergent, so that the low-temperature phase exhibits true long-range order. Most of the analytic calculations [6, 7] are performed in this gauge. In order to determine the critical behaviour of experimentally observable quantities, it is then necessary to transform back to the physical LC gauge. For thermodynamic quantities (e.g. internal energy and specific heat) and gauge-invariant quantities (e.g. the stiffness constants B and D and the twist and bend elastic constants K_2 and K_3), this does not pose any problem because these quantities exhibit the same critical behaviour in all gauges. However, the order-parameter correlations measured in X-ray scattering experiments are not gauge-invariant. Lubensky and co-workers [2, 18-20] have used a « decoupling approximation » to analyse the gauge-dependence of these correlations. The most interesting result of their analysis is the prediction that the exponents $\nu_{\parallel}^{\dagger}$ and ν_{\perp}^{\dagger} , which describe the growth of the correlation lengths associated with the physical order-parameter correlation functions may not be the same as the exponents ν_{\parallel} and ν_{\perp} which characterize the universality class of the transition. Combining the analysis of Lubensky *et al.* with anisotropic scaling, one obtains the following predictions [2] for the experimentally observable critical behaviour for the two universality classes mentioned earlier.

a) Isotropic : The specific heat in the critical region should behave as

$$C \sim |t|^{-\alpha_{XY}}, \quad (1)$$

where $t \equiv (T - T_c)/T_c$ and the subscript « XY » refers to the three-dimensional XY model. The asymmetry between $C(T \rightarrow T_c^+)$ and $C(T \rightarrow T_c^-)$ is expected to be opposite to that in the XY model. The fluctuation enhancements of the bend and twist elastic constants as $T \rightarrow T_c^+$ are predicted to have the form

$$\begin{aligned} \delta K_3 &\sim \xi_{\parallel}^{\dagger} \sim t^{-\nu_{XY}}, \\ \delta K_2 &\sim (\xi_{\perp}^{\dagger})^2 / \xi_{\parallel}^{\dagger} \sim t^{-\nu_{XY}}. \end{aligned} \quad (2)$$

Here, ξ_{\parallel}^f and ξ_{\perp}^s represent the correlation lengths in the SC gauge. Both these lengths diverge at the transition with the same exponent ν_{XY} . In the smectic phase, the stiffness constants B and D are expected to grow as

$$B \sim |t|^{\nu_{XY}}, \quad D \sim |t|^{\nu_{XY}}. \quad (3)$$

The values of the critical exponents of the three-dimensional XY model are [21] $\alpha_{XY} \approx -0.02$ and $\nu_{XY} \approx 0.67$. The X-ray correlation length exponent ν_{\parallel}^f is expected to be equal to ν_{XY} , whereas ν_{\perp}^s is predicted to show a crossover from ν_{XY} to $\nu_{XY}/2$ as $T \rightarrow T_c^+$.

b) Anisotropic: In this universality class, the SC gauge correlation lengths ξ_{\parallel}^f and ξ_{\perp}^s diverge as $T \rightarrow T_c$ with two different exponents, ν_{\parallel} and ν_{\perp} , with $\nu_{\parallel} = 2\nu_{\perp}$. The specific heat exponent α is given by

$$2 - \alpha = 2\nu_{\perp} + \nu_{\parallel} = 2\nu_{\parallel}. \quad (4)$$

The bend elastic constant is expected to diverge as the transition is approached from the nematic side:

$$\delta K_3 \sim t^{-\nu_{\parallel}}, \quad (5)$$

whereas K_2 is expected to remain finite at the transition. The stiffness constant B for layer dilations is predicted to exhibit a finite jump at $T = T_c$. The other stiffness constant D is expected to grow in the smectic phase as

$$D \sim |t|^{\nu_{\parallel}}. \quad (6)$$

In the anisotropic case, the decoupling approximation of Lubensky *et al.* breaks down [20] in the nematic phase and there are no reliable predictions about the behaviour of the X-ray correlation lengths as $T \rightarrow T_c^+$.

Neither of these two sets of theoretical predictions are in agreement with all the available experimental data. In spite of a large number of experimental studies of the NA transition, the situation remains somewhat confusing because the observed critical behaviour differs considerably from one system to another. To take an example, the reported values of the specific heat exponent α varies from -0.03 to 0.53 . Recently, some progress has been made towards understanding the origin of this non-universal behaviour. It has been demonstrated [22, 23] that the observed value of α increases continuously with decreasing width of the temperature range over which the nematic phase exists. The NA transition is first-order in nature in materials with very narrow nematic ranges. This implies the existence of a tricritical point [22, 23] which separates the region of continuous NA transitions from the region of first-order transitions. The observed dependence of α on the width of the nematic range can be qualitatively

understood in terms of cross-over effects arising from the presence of this tricritical point. In materials with broad nematic ranges, the observed values [24, 25] of α are close to the XY value. However, the asymmetry of the specific heat peak is found [24, 25] to be rather small, and to have the same sign as that observed in the λ -transition of helium. Both the correlation lengths ξ_{\parallel}^f and ξ_{\perp}^s measured in X-ray scattering experiments [1, 24, 26, 27] appear to exhibit single-power-law divergences as the transition is approached from the nematic side, although the cross-over form predicted by Lubensky *et al.* [2, 18] for the growth of ξ_{\perp}^s also provides adequate fits to the data in some cases. Except in materials which are close to the tricritical point, the observed values of ν_{\parallel}^f are 5-20% higher than ν_{XY} , and those of ν_{\perp}^s are 3-15% smaller than ν_{XY} . None of the existing theories of the NA transition is able to explain this behaviour. Several measurements [1, 24, 26-30] of the critical behaviour of the elastic constants have been reported in the literature. There seems to be some disagreement among the different experiments measuring the critical behaviour of the bend elastic constant K_3 . The experiments of Sprunt *et al.* [28] and Garland *et al.* [24] indicate that the exponent that characterizes the divergence of K_3 is the same as ν_{\parallel}^f . On the other hand, experiments performed by Gooden *et al.* [30] on the same materials suggest that the exponent for K_3 is universal and very close to ν_{XY} , while ν_{\parallel}^f varies from one material to another. The latter results would be consistent with an inverted XY transition. The twist elastic constant K_2 also diverges [1, 28, 29] at the transition. This divergence is clearly inconsistent with a critical point with $\nu_{\parallel} = 2\nu_{\perp}$. The reported values [1, 28, 29] of the exponent for K_2 are somewhat smaller than ν_{XY} , although there are indications [29] that the value of this exponent increases with increasing width of the nematic range. The critical behaviour of the stiffness constants B and D in the smectic phase has not been studied as extensively. The available data [1, 26, 27, 31-33] indicate an exponent of $\approx 0.3-0.4$ for B and ≈ 0.5 for D . These values are inconsistent with the predictions of both the inverted XY and the anisotropic universality classes.

The failure of theories based on the de Gennes model to account for all the available experimental results raises questions about the validity of this model. A recent experimental study by Chan *et al.* [34] claims to have provided evidence suggesting that the de Gennes free energy is not adequate for quantitative predictions about the NA transition. In this experiment, the temperature dependence of finite-range order-parameter correlations is measured from the integrated X-ray intensity. The authors argue that the de Gennes form of the free energy implies that the temperature-dependence of

the singular part of this quantity should be described by the same exponent as that for the internal energy. The experimental results do not agree with this prediction. This discrepancy is interpreted as evidence suggesting that the de Gennes model misses some essential physics of the NA transition.

This summary of the available theoretical and experimental information about the NA transition clearly shows that the present understanding of this phase transition is far from complete. In this paper, we describe the results of a Monte Carlo simulation of the critical behaviour of a lattice version of the de Gennes model in three dimensions. Two main questions were addressed in this numerical study. These are : 1) does the de Gennes model provide an adequate description of the NA transition ? and 2) what is the universality class of the phase transition in the de Gennes model ? The main results are described below. A summary of these results was reported earlier in a letter [35].

Concerning the first question, I found that the simulations qualitatively reproduce several features observed in experiments. The model exhibits a second-order phase transition with the specific heat exponent α close to zero. The temperature-asymmetry of the specific heat peak is similar to what is observed in experiments on materials for which $\alpha \approx 0$. The correlation lengths associated with the order-parameter correlation function show anisotropic growth in the nematic phase. A peculiar feature of the experimentally observed X-ray scattering profile is reproduced in the simulation. Short-range order-parameter correlations show a temperature-dependence similar to that observed in the experiment of reference [34]. Because of the smallness of the size of the samples simulated in this study, accurate determinations of the values of the critical exponents were not possible. For this reason, a quantitative comparison with experimental results cannot be made at this stage. However, the fact that the qualitative behaviour observed in the simulations is remarkably similar to what is seen in experiments provides strong support to the validity of the de Gennes model.

In order to determine the universality class of the transition, I calculated the correlation functions in the SC gauge. Since all experiments are restricted to the physical LC gauge, a numerical simulation is the only way of « experimentally » studying the critical behaviour in the SC gauge. The results strongly indicate an isotropic critical point. For both small and large values of the splay elastic constant K_1 , the ratio of $\xi_{\parallel}^s/\xi_{\perp}^s$ remains very nearly constant as the transition is approached from the nematic side. The observed behaviour of the bend and twist elastic constants is consistent with this conclusion. The gauge-dependence of the correlation function is found to be well-described by the decoupling ap-

proximation proposed by Lubensky *et al.* These results imply that at the NA transition, all thermodynamic and gauge-invariant quantities should exhibit inverted XY behaviour, whereas the X-ray correlation lengths should show a crossover [2, 18] from isotropic to anisotropic behaviour as $T \rightarrow T_c^+$.

The rest of the paper is organized as follows. Section 2 contains a definition of the model studied in this work and a description of the numerical procedure used in the Monte Carlo simulation. The results are described in detail in section 3. Section 4 contains a summary of the main results and a few concluding remarks.

2. Model and simulation procedure.

The model studied in this work is a discretized version of the three-dimensional de Gennes model. It is defined on a three-dimensional simple cubic lattice with periodic boundary conditions. The lattice sites are labelled by the radius vectors

$$\mathbf{r}_i = \sum_{\mu=x,y,z} n_{i\mu} \hat{\mu} . \quad (7)$$

Here, $\hat{\mu}$ represents an unit vector in the μ -direction and $n_{i\mu} = 1, 2, \dots, L$, where L is the linear size of the lattice. The smectic order is described by an angular (phase) variable, $\theta(\mathbf{r}_i)$, defined at each site ($-\pi \leq \theta(\mathbf{r}_i) \leq \pi$). In the continuum de Gennes model, the smectic order-parameter has an amplitude as well as a phase. In the lattice model, fluctuations in the amplitude are not allowed. This constraint corresponds to the extreme type-II limit [17] in the superconducting analogy. Since liquid crystals exhibiting a continuous NA transition are expected to be in the type-II regime, the fixed-length constraint is justified. Fluctuations in the director field are represented by real variables, $A_x(\mathbf{r}_i)$ and $A_y(\mathbf{r}_i)$, with $A_z(\mathbf{r}_i) = 0$. These variables are defined on the links between adjacent lattice sites. In terms of these variables, the Hamiltonian of the model is given by

$$\begin{aligned} H = & \sum_{i=1}^N \left\{ B_0 [1 - \cos(\Delta_z \theta(\mathbf{r}_i))] + \right. \\ & + D_0 \sum_{\mu=x,y} [1 - \cos(\Delta_{\mu} \theta(\mathbf{r}_i) - A_{\mu}(\mathbf{r}_i))] \\ & + \frac{1}{2} K_1^0 \left[\sum_{\mu=x,y} \Delta'_{\mu} A_{\mu}(\mathbf{r}_i) \right]^2 \\ & + \frac{1}{2} K_2^0 [\Delta_x A_y(\mathbf{r}_i) - \Delta_y A_x(\mathbf{r}_i)]^2 \\ & \left. + \frac{1}{2} K_3^0 \sum_{\mu=x,y} [\Delta_z A_{\mu}(\mathbf{r}_i)]^2 \right\} . \quad (8) \end{aligned}$$

In equation (8), Δ_{μ} and Δ'_{μ} represent right and left lattice derivatives, respectively :

$$\begin{aligned}\Delta_\mu f(\mathbf{r}_i) &\equiv f(\mathbf{r}_i + \hat{\boldsymbol{\mu}}) - f(\mathbf{r}_i), \\ \Delta'_\mu f(\mathbf{r}_i) &\equiv f(\mathbf{r}_i) - f(\mathbf{r}_i - \hat{\boldsymbol{\mu}}).\end{aligned}\quad (9)$$

The z -axis is chosen to lie along the direction of smectic ordering. B_0 and D_0 are the « bare » stiffness constants, and K_1^0 , K_2^0 and K_3^0 represent the « bare » Frank elastic constants [10] for splay, twist and bend distortions, respectively. The length scale is chosen such that the wavenumber associated with the smectic order is equal to unity. The total number of sites on the lattice is $N = L^3$.

It was shown earlier [14] that the partition function of the Villain version of this model maps exactly onto that of a system of interacting dislocation loops. Thus, this model describes the same physics as the dislocation melting theories. This model is also closely related, *via* a gauge transformation, to the lattice superconductor model studied in reference [16]. A gauge transformation for the lattice model is defined by the change of variables, $\theta \rightarrow \phi$ and $A \rightarrow A'$, with

$$\begin{aligned}\theta(\mathbf{r}_i) &= \phi(\mathbf{r}_i) - L(\mathbf{r}_i), \\ A_\mu(\mathbf{r}_i) &= A'_\mu(\mathbf{r}_i) - \Delta_\mu L(\mathbf{r}_i), \quad \mu = x, y, z,\end{aligned}\quad (10)$$

where the variables $L(\mathbf{r}_i)$ are to be determined from a gauge condition. In particular, the SC gauge is defined by the condition

$$\sum_{\mu=x,y,z} \Delta_\mu A'_\mu(\mathbf{r}_i) = 0 \quad \text{for all } i, \quad (11)$$

which implies that the variables $L(\mathbf{r}_i)$ are determined from the set of equations

$$\Delta^2 L(\mathbf{r}_i) + \sum_{\mu=x,y} \Delta_\mu A_\mu(\mathbf{r}_i) = 0. \quad (12)$$

It is easy to check that if K_1^0 is equal to zero, then a transformation to the SC gauge reduces the Hamiltonian of equation (8) to an anisotropic version of the lattice superconductor model of reference [16], which is believed to exhibit an inverted XY transition. The present work may, therefore, be viewed as a study of the effects of the splay term on the nature of the phase transition. I chose the values $B_0 = D_0 = 5.0$, $K_2^0 = K_3^0 = 1.0$ in order to remain close in parameter space to the simulation described in reference [16]. The role of the splay term was investigated by simulating the thermodynamic behaviour of the model for two different values (0.5 and 5.0) of K_1^0 .

The standard Metropolis algorithm [36] was used in the Monte Carlo simulations. The model of equation (8) involves three sets of variables, $\theta(\mathbf{r}_i)$, $A_x(\mathbf{r}_i)$ and $A_y(\mathbf{r}_i)$. Most of the results reported in this paper were obtained from simulations in which these variables were updated one at a time. A Monte

Carlo update of a variable consists of the following three steps. First, a value of the attempted change is chosen at random from within a certain range. Then, the energy change, ΔE , associated with the attempted update is calculated. If $\Delta E \leq 0$, the change is accepted. If $\Delta E > 0$, the change is accepted with a probability $\exp(-\Delta E/T)$. The range of values of the attempted change was adjusted to keep the acceptance ratio close at 0.5. The simulations were performed on the CRAY 1 computer at the Minnesota Supercomputer Institute. In order to take advantage of the vectorizing capability of the CRAY, I divided the lattice into four sublattices in such a way that the calculation of ΔE for the updating of a variable on a particular sublattice does not involve any other variable of the same set belonging to the same sublattice. All the variables of a particular set belonging to one of the four sublattices could then be updated simultaneously in a single vectorized step. Simulations were carried out for samples with $L = 6, 8$ and 10 . Standard methods were used in the calculation of equilibrium averages. Typically, 1 000-2 000 Monte Carlo steps per variable were used for equilibration, and 5 000-10 000 steps per variable were used for calculating averages. A 10 000-step run for a $L = 10$ sample used approximately 200 s of c.p.u. time of the CRAY 1.

Due to reasons which will be explained in the next section, correlation functions in the SC gauge were calculated from simulations in which the constraints

$$\sum_{n_{ix}=1}^L A_x(n_{ix} \hat{\mathbf{x}} + n_{iy} \hat{\mathbf{y}} + n_{iz} \hat{\mathbf{z}}) = 0 \quad (13a)$$

and

$$\sum_{n_{iy}=1}^L A_y(n_{ix} \hat{\mathbf{x}} + n_{iy} \hat{\mathbf{y}} + n_{iz} \hat{\mathbf{z}}) = 0 \quad (13b)$$

were imposed on the allowed values of the variables $A_\mu(\mathbf{r}_i)$. These restrictions were implemented by using an updating procedure similar to the one used in simulations of Ising models with conserved total magnetization. In this procedure, the variables $A_\mu(\mathbf{r}_i)$ are updated in pairs. Whenever a variable $A_\mu(\mathbf{r}_i)$ is changed by an amount δ , the nearest-neighbour variable $A_\mu(\mathbf{r}_i + \hat{\boldsymbol{\mu}})$ is also changed by an amount $(-\delta)$. If the initial configuration satisfies the constraints (13a) and (13b), then all subsequent configurations generated by successive applications of this algorithm also do so. A computer program implementing this algorithm was vectorized by breaking the lattice up into L sublattices. Calculations of correlation functions in the SC gauge were straightforward, but tedious. The solutions of the set of equations (12) can be written as

$$L(\mathbf{r}_i) = \sum_{j=1}^N M_{ij} \sum_{\mu} \Delta_\mu A_\mu(\mathbf{r}_j), \quad (14)$$

where the elements of the $N \times N$ matrix \mathbf{M} depend only on the type of the lattice. This matrix was calculated and stored in the memory of the computer. The values of $L(\mathbf{r}_i)$ corresponding to a particular configuration of $A_\mu(\mathbf{r}_i)$ were then calculated from equation (14). The large amount of computer time required for this procedure restricted the calculation of SC gauge correlation functions to samples with $L \leq 8$.

3. Results.

In this section, the results obtained from the numerical simulations are described in detail and compared, when appropriate, with theoretical predictions and experimental observations. The simulations did not show any indication of a first-order phase transition. Results obtained from heating and cooling runs were identical within statistical uncertainties, indicating the absence of any hysteresis. I did not find any significant difference between the critical properties for the two different values of K_1^0 ($K_1^0 = 0.5$ and 5.0) considered in this work. For this reason, only the results for $K_1^0 = 0.5$ are shown in most cases. Unless otherwise indicated, the results presented below were obtained from simulations in which no restriction was imposed on the variables.

3.1 SPECIFIC HEAT. — The specific heat C was calculated from a numerical differentiation of the internal energy E with respect to the temperature T , and also from the fluctuations of the internal energy. The values obtained from these two different procedures were in agreement within the error bars (≈ 5 - 10 %). The results for samples with $L = 6, 8$ and 10 are shown in figure 1. The data points shown were obtained from a numerical calculation of dE/dT . The specific heat peaks at approximately the same temperature for the three different values of L . The height of the peak increases with L , as expected for a continuous phase transition. Because of the smallness of sample-size, an accurate determination of the specific-heat exponent α is not possible. However, it is possible to show that the observed behaviour of C is consistent with α being close to zero. For a system with $\alpha = 0$, the specific heat in the critical region is expected [37] to have the form

$$C = -A \ln |t| - \frac{1}{2} D A t / |t| + B, \quad (15)$$

where $t \equiv (T - T_c)/T_c$ and A, B and D are constants. Measurements [37] at the λ -point of helium indicate that the value of the asymmetry parameter D is close to 4 in the three-dimensional XY model. Thus, the value of D expected for an inverted XY transition is close to (-4) . A plot of C versus $\ln(|T - T^*|/T^*)$ where $T^* = 6.15$ is the temperature at the specific heat peak for $L = 10$ and

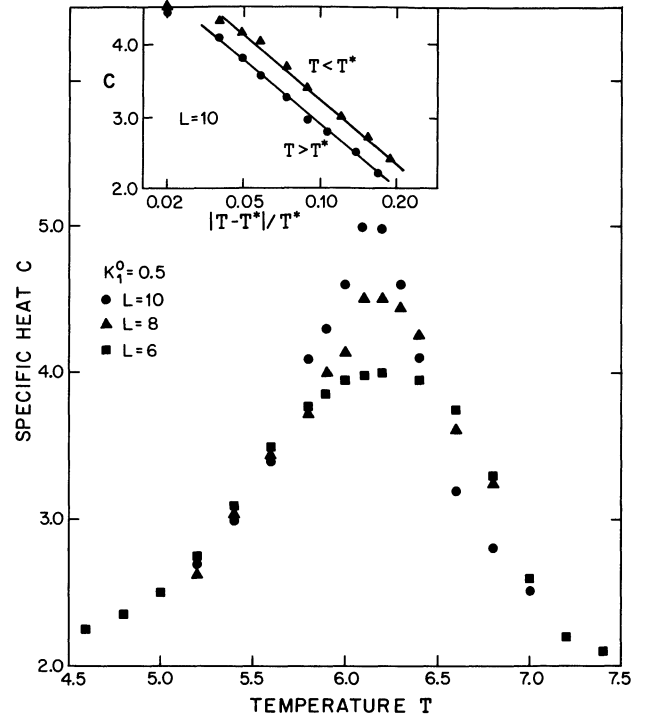


Fig. 1. — Variation of the specific heat C with temperature T for $K_1^0 = 0.5$. The inset shows semilog plots of C for the $L = 10$ sample vs. $|T - T^*|/T^*$, where $T^* (= 6.15)$ is the temperature at the specific heat peak.

$K_1^0 = 0.5$ is shown in the inset of figure 1. It is clear that the data points are consistent with the form of equation (15). The size-dependence of the height of the specific heat peak is also consistent with the prediction of finite-size scaling [38] with $\alpha \approx 0$. However, the asymmetry parameter D appears to be rather small (≈ 0.25) and its sign is the same as that expected for the regular XY transition. A qualitatively similar behaviour of the specific heat near the NA transition has been observed [24, 25] in experiments on materials for which $\alpha \approx 0$. Thus, the inversion of the temperature axis expected for an isotropic NA transition does not show up either in the simulation or in experiments. Crossover effects and/or corrections to scaling arising from the K_1^0 term may account for this discrepancy. A theoretical understanding of these effects requires further study. It should be noted that a value of α close to zero does not rule out an anisotropic critical point because the values of the critical exponents for this universality class are not known theoretically.

3.2 X-RAY CORRELATION FUNCTIONS. — An intriguing feature of the NA transition is the anisotropic critical behaviour of the order-parameter correlation lengths measured in X-ray scattering experiments [1, 24, 26, 27]. In the simulations, I calculated the order-parameter correlation functions, $g(l)$, defined by

$$g(\mathbf{l}) = \frac{1}{N} \sum_i \langle \cos [\theta(\mathbf{r}_i + \mathbf{l}) - \theta(\mathbf{r}_i)] \rangle, \quad (16)$$

where $\langle \dots \rangle$ represents a thermal (Monte Carlo) average and \mathbf{l} is a lattice vector. The discrete Fourier transforms of $g(\mathbf{l})$ are defined as

$$g(\mathbf{k}) = \sum_{\mathbf{l}} e^{i\mathbf{k} \cdot \mathbf{l}} g(\mathbf{l}), \quad (17)$$

with $\mathbf{k} = \frac{2\pi}{L} (\hat{x}m_x + \hat{y}m_y + \hat{z}m_z)$, where m_μ , $\mu = x, y, z$, are integers with $-L/2 < m_\mu \leq L/2$. It is clear from the definition of the model, equation (8), that $g(\mathbf{k})$ is the discrete analog of the X-ray scattering intensity $I(\mathbf{k} + q_0 \hat{z})$ where q_0 is the wave number associated with the smectic ordering. In order to determine the X-ray correlation lengths ξ_{\parallel}^x and ξ_{\perp}^x in the nematic phase, I used a procedure similar to the one used in the analysis of X-ray scattering data. This procedure consists of fitting the scattering profile to a Lorentzian of the form

$$I(\mathbf{k} + q_0 \hat{z}) = \frac{T\chi}{1 + (\xi_{\parallel}^x k_z)^2 + (\xi_{\perp}^x k_{\perp})^2}, \quad (18)$$

where χ is the order-parameter susceptibility and $k_{\perp}^2 = k_x^2 + k_y^2$. Experimentally, it is found [1, 24, 26, 27] that for \mathbf{k} is the \parallel (z) direction, this form provides a good fit to the data. However, for \mathbf{k} is the \perp (xy) plane, the scattering intensity falls off faster than a Lorentzian, and a fourth-order term, $c(\xi_{\perp}^x k_{\perp})^4$, has to be included in the denominator of equation (18) in order to obtain adequate fits to the data. The coefficient c is found to be weakly temperature dependent, with values in the range 0.05-0.20. The presence of the $(\xi_{\perp}^x)^4$ factor in the definition of this fourth-order term implies that the relative importance of this term increases as $T \rightarrow T_c^+$. A satisfactory explanation of this behaviour is not yet available. It has been suggested [1, 39] that the k_{\perp}^4 term is a manifestation of the divergent fluctuations in the phase of the smectic order parameter.

The behaviour of $g(\mathbf{k})$ calculated in the simulations is very similar to the experimentally observed behaviour described above. The discrete analog of equation (18) is

$$g(\mathbf{k}) = \frac{T\chi}{1 + (\xi_{\parallel}^x)^2 |\alpha_z(\mathbf{k})|^2 + (\xi_{\perp}^x)^2 |\alpha_{\perp}(\mathbf{k})|^2}, \quad (19)$$

where

$$\alpha_{\mu}(\mathbf{k}) \equiv 1 - e^{i\mathbf{k} \cdot \boldsymbol{\mu}}, \quad \mu = x, y, z, \quad (20)$$

and

$$|\alpha_{\perp}(\mathbf{k})|^2 \equiv |\alpha_x(\mathbf{k})|^2 + |\alpha_y(\mathbf{k})|^2. \quad (21)$$

For \mathbf{k} in the z -direction, the data for $g(\mathbf{k})$ are well-described by equation (19). As shown in figure 2,

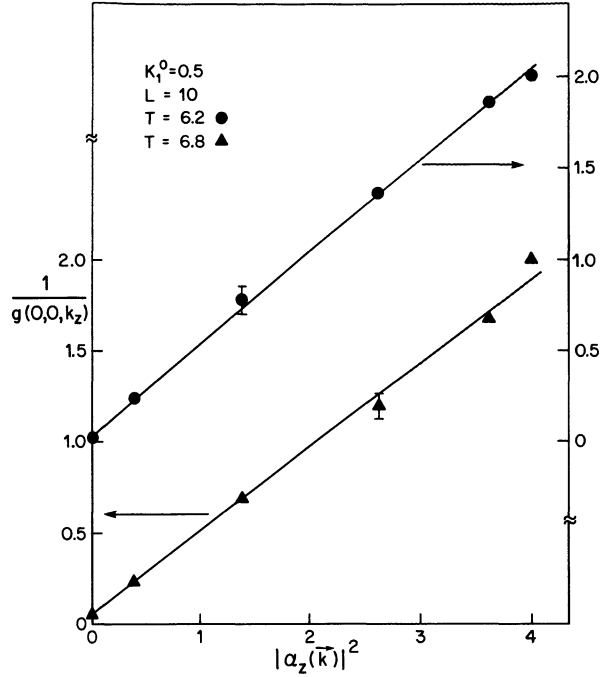


Fig. 2. — Plots of the inverse of $g(\mathbf{k})$, the Fourier transform of the order-parameter correlation function ($L = 10$, $K_1^0 = 0.5$) vs. $|\alpha_z(\mathbf{k})|^2$ (see text) for \mathbf{k} in the parallel (z) direction at $T = 6.8$ (triangles, left scale) and $T = 6.2$ (circles, right scale). The solid lines are best fits to the Lorentzian form of equation (19).

plot of $[g(\mathbf{k})]^{-1}$ versus $|\alpha_z(\mathbf{k})|^2$ can be fitted quite well by straight lines for all $T > T^*$. However, for \mathbf{k} in the xy -plane, plots of $[g(\mathbf{k})]^{-1}$ versus $|\alpha_{\perp}(\mathbf{k})|^2$ show considerable upward curvature, and it is necessary to include a fourth-order term, $c|\alpha_{\perp}(\mathbf{k})|^4$, in the denominator of equation (19) for good fits to the data. Results for two different temperatures are shown in figure 3. It is apparent that the curvature (and consequently, the value of c) increases as T approaches T^* . An explanation of this behaviour will be suggested in section 3.5 below. Here, the results for ξ_{\parallel}^x and ξ_{\perp}^x obtained from the fits are described. The inset of figure 3 shows the observed temperature-dependence of the ratio $\xi_{\parallel}^x/\xi_{\perp}^x$ for $L = 10$, $K_1^0 = 0.5$. The results clearly exhibit an anisotropic growth of the two correlation lengths as the transition is approached from the nematic side. Large fluctuations in the value of the susceptibility χ made an accurate determination of the absolute values of ξ_{\parallel}^x and ξ_{\perp}^x impossible, although the values of $(\xi_{\parallel}^x)^2/\chi$ and $(\xi_{\perp}^x)^2/\chi$ and therefore, the ratio $\xi_{\parallel}^x/\xi_{\perp}^x$ could be determined with fair accuracy from the fits similar to the ones shown in figure 2 and figure 3. Because of this reason and the smallness of sample-size, I was not able to obtain any reliable estimate of the values of the exponents associated with the growth of the X-ray correlation lengths.

It is, in principle, possible to extract the values of

the stiffness constants in the smectic phase form the data for $\tilde{g}(\mathbf{l})$. A harmonic « spin-wave » analysis [2, 9] predicts the following form for $g(\mathbf{l})$ in the smectic phase :

$$g(\mathbf{l}) = \exp \left[-\frac{1}{N} \sum_{\mathbf{k}} \Lambda(\mathbf{k})(1 - \cos \mathbf{k} \cdot \mathbf{l}) \right], \quad (22)$$

where

$$\Lambda(\mathbf{k}) = \frac{T[K_1 |\alpha_{\perp}(\mathbf{k})|^2 + D + K_3 |\alpha_z(\mathbf{k})|^2]}{B |\alpha_z(\mathbf{k})|^2 [D + K_3 |\alpha_z(\mathbf{k})|^2] + |\alpha_{\perp}(\mathbf{k})|^2 [BK_1 |\alpha_z(\mathbf{k})|^2 + DK_1 |\alpha_{\perp}(\mathbf{k})|^2 + DK_3 |\alpha_z(\mathbf{k})|^2]}. \quad (23)$$

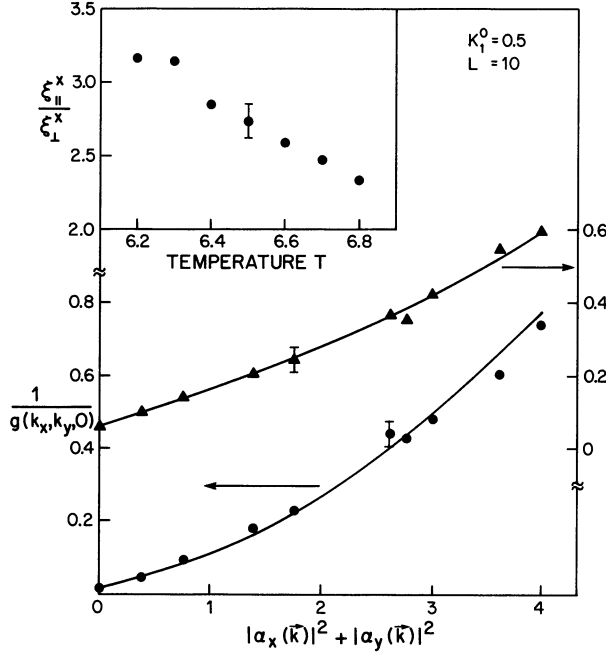


Fig. 3. — Plots of the inverse of $g(\mathbf{k})$ vs. $|\alpha(\mathbf{k})|^2$ for $L = 10$, $K_1^0 = 0.5$, and \mathbf{k} in the perpendicular (xy) plane at $T = 6.8$ (triangles, right scale) and $T = 6.2$ (circles, left scale). The solid lines are the best fits to the form of equation (19) with an $|\alpha(\mathbf{k})|^4$ term included in the denominator (see text). The inset shows the temperature dependence of the ratio of the two X-ray correlation lengths for $L = 10$, $K_1^0 = 0.5$.

The stiffness constants, B and D , and the elastic constants, K_1 , K_2 and K_3 , appearing in equation (23) are the renormalized ones defined at long wavelengths. They are, in general, different from the « bare » ones denoted by the subscript or superscript 0. It follows from equation (22) that

$$h(\mathbf{k}) \equiv - \sum_{\mathbf{l}} \ln [g(\mathbf{l})] e^{i\mathbf{k} \cdot \mathbf{l}} = \Lambda(\mathbf{k}). \quad (24)$$

In the simulation, the quantities $h(\mathbf{k})$ were calculated. I tried to fit the \mathbf{k} -dependence of $h(\mathbf{k})$ to the form of equation (23), with K_1 , K_2 and K_3 fixed at their « bare » values. This procedure works quite well for temperatures less than $\approx 0.9 T^*$. A typical set of fits are shown in figure 4. The values of B and D obtained from such fits are found to be substantially smaller than their « bare » values over the temperature range studied. Both B and D decrease

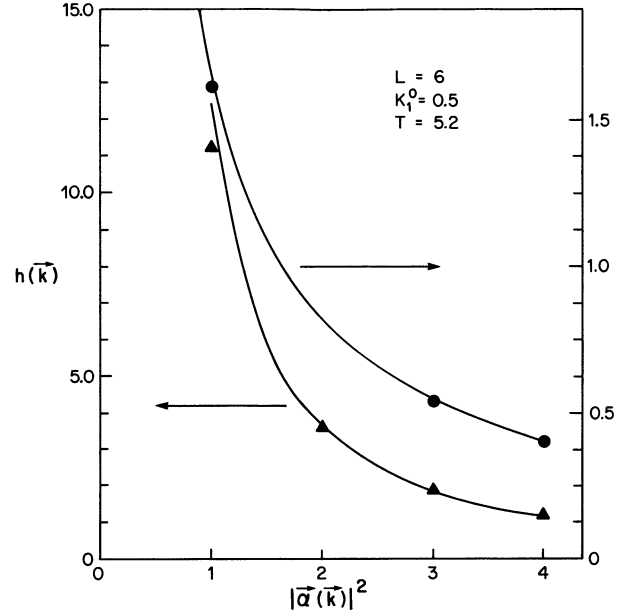


Fig. 4. — Plots of $h(\mathbf{k})$ defined in equation (24) vs. $|\alpha(\mathbf{k})|^2$ for $L = 6$, $K_1^0 = 0.5$, $T = 5.2$, and \mathbf{k} in the parallel direction (circles, right scale), and in the perpendicular plane (triangles, left scale). The solid lines represent the behaviour expected from equation (23) with $B = 3.2$, $D = 2.5$, $K_1 = 0.5$ and $K_2 = K_3 = 1.0$.

with increasing temperature, as expected, with D always smaller than B . For $T > 0.9 T^*$, large critical fluctuations in $g(\mathbf{l})$ make an accurate determination of $h(\mathbf{k})$ difficult. Also, the quality of the fit to the form of equation (23) deteriorates rapidly as $T \rightarrow T^*$. Letting K_2 and K_3 be different from the « bare » values does not produce any substantial improvement of the fits. For these reasons, it was not possible to obtain reliable results on the growth of B and D in the critical region.

3.3 CORRELATION FUNCTIONS FOR DIRECTOR FLUCTUATIONS. — As discussed in the Introduction, the anisotropic behaviour of the X-ray correlation lengths does not necessarily imply that the NA transition is described by anisotropic scaling. The true nature of the critical point is expected to manifest itself in the behaviour of gauge-invariant quantities such as the stiffness constants B and D , and the renormalized Frank elastic constants K_2 and K_3 . These quantities can be obtained from measure-

ments of the correlation functions for director fluctuations. The director field correlation functions for the model of equation (8) are defined as

$$D_{\mu\nu}(\mathbf{l}) = \frac{1}{N} \sum_i \langle A_\mu(\mathbf{r}_i) A_\nu(\mathbf{r}_i + \mathbf{l}) \rangle, \quad \mu, \nu = x, y. \quad (25)$$

$$D_{\mu\mu}(\mathbf{k}) = \begin{cases} \frac{T}{K_1 |\alpha_\nu(\mathbf{k})|^2}, & \mu = x, y; \quad \nu = \mu, \\ \frac{T}{K_2 |\alpha_\nu(\mathbf{k})|^2}, & \mu = x, y; \quad \nu \neq \mu, \nu \neq z, \\ \frac{T}{K_3 |\alpha_\nu(\mathbf{k})|^2}, & \mu = x, y; \quad \nu = z. \end{cases} \quad (26a)$$

$$D_{\mu\mu}(\mathbf{k}) = \begin{cases} \frac{T}{K_1 |\alpha_\nu(\mathbf{k})|^2}, & \mu = x, y; \quad \nu = \mu, \\ \frac{T}{K_2 |\alpha_\nu(\mathbf{k})|^2}, & \mu = x, y; \quad \nu \neq \mu, \nu \neq z, \\ \frac{T}{K_3 |\alpha_\nu(\mathbf{k})|^2}, & \mu = x, y; \quad \nu = z. \end{cases} \quad (26b)$$

$$D_{\mu\mu}(\mathbf{k}) = \begin{cases} \frac{T}{K_1 |\alpha_\nu(\mathbf{k})|^2}, & \mu = x, y; \quad \nu = \mu, \\ \frac{T}{K_2 |\alpha_\nu(\mathbf{k})|^2}, & \mu = x, y; \quad \nu \neq \mu, \nu \neq z, \\ \frac{T}{K_3 |\alpha_\nu(\mathbf{k})|^2}, & \mu = x, y; \quad \nu = z. \end{cases} \quad (26c)$$

Since twist and bend distortions are expelled from the smectic-A phase whereas splay distortions are allowed, the elastic constants K_2 and K_3 are expected to show fluctuation enhancements as the transition is approached from the nematic side, and K_1 is expected to remain unchanged from its bare value, K_1^0 . The enhancements of K_2 and K_3 can be related [40] to the correlation lengths ξ_{\parallel}^s and ξ_{\perp}^s defined in the introduction :

$$\delta K_2 \equiv K_2 - K_2^0 = T(\xi_{\perp}^s)^2 / 24 \pi \xi_{\parallel}^s, \quad (27a)$$

$$\delta K_3 \equiv K_3 - K_3^0 = T \xi_{\parallel}^s / 24 \pi. \quad (27b)$$

Since, according to equation (27), $\delta K_3 / \delta K_2 \sim (\xi_{\parallel}^s / \xi_{\perp}^s)^2$, measurements of the temperature-dependence of this ratio should, in principle, settle the question of whether the NA transition is described by anisotropic scaling or not. In the smectic phase, equations (26b) and (26c) are modified to the form

$$D_{\mu\mu}(\mathbf{k}) = \begin{cases} \frac{T}{D + K_2 |\alpha_\nu(\mathbf{k})|^2}, & \mu = x, y; \quad \nu \neq \mu; \quad \nu \neq z, \\ \frac{T}{D + K_3 |\alpha_\nu(\mathbf{k})|^2}, & \mu = x, y; \quad \nu = z. \end{cases} \quad (28a)$$

$$D_{\mu\mu}(\mathbf{k}) = \begin{cases} \frac{T}{D + K_2 |\alpha_\nu(\mathbf{k})|^2}, & \mu = x, y; \quad \nu \neq \mu; \quad \nu \neq z, \\ \frac{T}{D + K_3 |\alpha_\nu(\mathbf{k})|^2}, & \mu = x, y; \quad \nu = z. \end{cases} \quad (28b)$$

The behaviour observed in the simulations is in good agreement with equations (26) and (28). Plots of $T/D_{\mu\mu}(\mathbf{k})$ versus $|\alpha_\nu(\mathbf{k})|^2$ are well-described by straight lines for small values of k . At high temperatures, the straight-line fits to the data pass through the origin, whereas for T less than $\sim 1.1 T^*$, the intercepts at $k = 0$ are finite. Typical results are shown in figure 5. Values of K_1, K_2, K_3 and D were extracted from such fits. As expected, K_1 remains equal to K_1^0 through the transition, and both K_2 and K_3 exhibit small but detectable enhancements in the critical region. The results for $\delta K_1, \delta K_2$ and δK_3 are shown in the inset of figure 5. There is no indication of any increase in the value of $\delta K_3 / \delta K_2$ as the transition temperature is approached from above. This ratio, in fact, decreases as $T \rightarrow T^*$. Also, the observed values of this ratio are substantially smaller than those of $(\xi_{\parallel}^s / \xi_{\perp}^s)^2$ obtained from X-ray correlation functions (see Sect. 3.2) at all temperatures. These results are consistent with an

isotropic critical point. However, the evidence for isotropic behaviour is far from being conclusive. At temperatures much higher than T^* , the values of δK_2 and δK_3 are very small and their ratio can not be determined accurately. For $T \approx T^*$, on the other hand, both ξ_{\parallel}^s and ξ_{\perp}^s are expected to saturate at values $\approx L/2$, irrespective to the nature of the critical point. Therefore, the observed result, $\delta K_3 / \delta K_2 \approx 1$ near $T = T^*$, can not really differentiate between isotropic and anisotropic critical behaviour. Furthermore, equations (26) and (27) describe the behaviour in the long-wavelength hydrodynamic ($k\xi \ll 1$) limit. Because of the smallness of sample-size, the applicability of these equations to the results of the simulation is questionable, especially at temperatures close to T^* . This is perhaps the reason why the observed values of δK_2 and δK_3 at $T \approx T^*$ are somewhat smaller than the values expected from equation (27) with $\xi_{\parallel}^s \approx \xi_{\perp}^s \approx L/2$. For these reasons, it is difficult to draw any firm

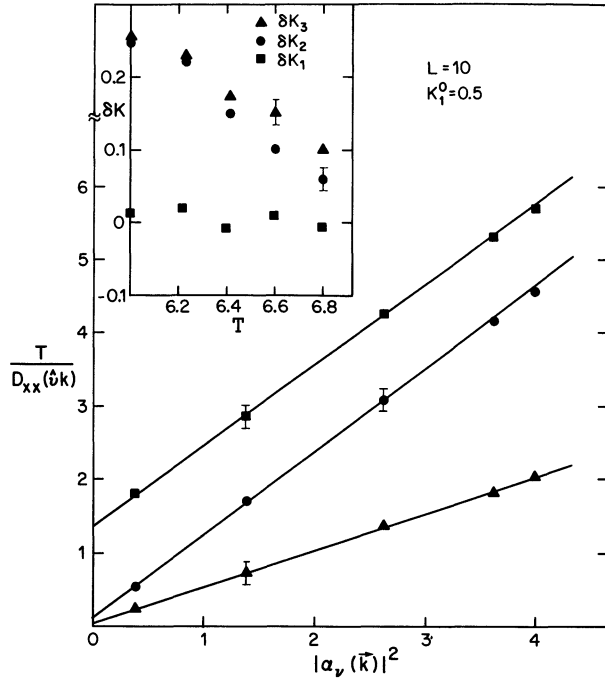


Fig. 5. — Plots of $T/D_{xx}(\delta k)$ (see text) vs. $|\alpha_\nu(\mathbf{k})|^2$ for $L = 10$, $K_1^0 = 0.5$ [triangles: $\nu = x$, $T = 6.4$; circles: $\nu = y$, $T = 6.4$; squares: $\nu = y$, $T = 5.7$]. The straight lines are the best fits. The inset shows the temperature dependence of the fluctuation enhancements of the Frank constants in the nematic phase.

conclusion about the nature of the NA critical point from the results for $D_{\mu\nu}$. Simulations of much larger samples would be necessary to clarify this aspect.

The values of D obtained from the data on director fluctuations agree with those calculated at low temperatures from X-ray correlation functions (see Sect. 3.2 above). As expected, D decreases with increasing temperature and goes to zero at $T \approx 1.1 T^*$. No sharp feature is noticeable at $T = T^*$. Because of this finite-size rounding, no attempt was made to extract a value of the critical exponent that describes the vanishing of D at the transition.

3.4 SHORT-RANGE ORDER-PARAMETER CORRELATIONS. — As mentioned in the introduction, the results of a recent experiment [34] on the critical behaviour of short-range order-parameter correlations have been interpreted as evidence indicating the inadequacy of the de Gennes model in describing quantitatively the physics of the NA transition. This issue was investigated in the simulation by calculating the nearest-neighbour correlation functions

$$g_{nn}^{\parallel} = \frac{1}{N} \sum_i \langle \cos [\theta(\mathbf{r}_i + \hat{\mathbf{z}}) - \theta(\mathbf{r}_i)] \rangle, \quad (29)$$

$$g_{nn}^{\perp} = \frac{1}{2N} \sum_i \sum_{\mu=x,y} \langle \cos [\theta(\mathbf{r}_i + \hat{\boldsymbol{\mu}}) - \theta(\mathbf{r}_i)] \rangle.$$

According to the arguments presented in refer-

ence [34], the temperature-dependence of the singular part of the quantity

$$g_{nn} = g_{nn}^{\parallel} + 2 g_{nn}^{\perp} \quad (30)$$

should be described by the same exponent as the internal energy. I tested this prediction by calculating the temperature derivative, dg_{nn}/dT , from a numerical differentiation of the Monte Carlo data for $g_{nn}(T)$. The results for $L = 10$, $K_1^0 = 0.5$ are shown in figure 6 as a plot of dg_{nn}/dT versus $\ln[|T - T^*|/T^*]$. From a comparison of this plot with the one shown in the inset of figure 1, it appears that the temperature-dependence of g_{nn} in the critical region is more singular than that of the internal energy. This behaviour is qualitatively similar to that

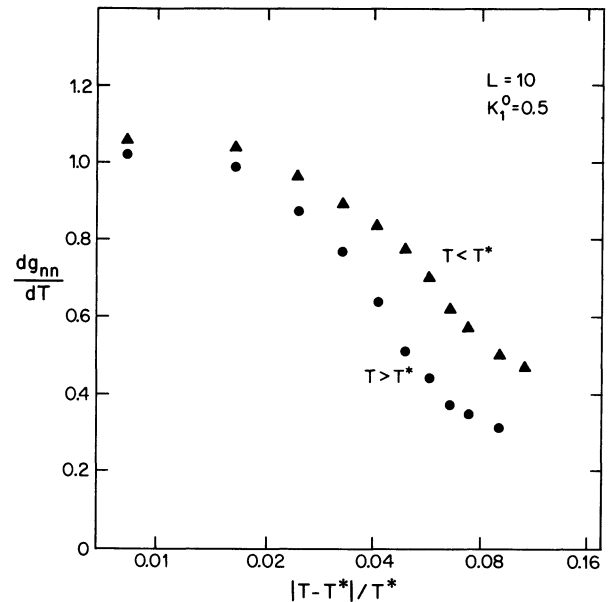


Fig. 6. — Semilog plots of the temperature derivative of g_{nn} , the nearest-neighbour order-parameter correlation function ($L = 10$, $K_1^0 = 0.5$) vs. $|T - T^*|/T$ where T^* ($= 6.15$) is the temperature at the specific heat peak.

observed in the experiment of Chan *et al.* [34] who found that the exponent that characterizes the dependence of short-range correlations on the reduced temperature is smaller than $(1 - \alpha)$. The results of this simulation, therefore, tend to support the validity of the de Gennes model, and appear to disagree with the theoretical arguments of reference [34]. This disagreement may be related to the fact that the order-parameter correlation functions are not gauge-invariant whereas the internal energy is. It is clear from equation (8) that the gauge-invariant nearest-neighbour correlation g'_{nn} defined by

$$g'_{nn} = g_{nn}'' + \frac{1}{N} \sum_i \sum_{\mu=x,y} \langle \cos [\theta(\mathbf{r}_i + \hat{\boldsymbol{\mu}}) - \theta(\mathbf{r}_i) - A_{\mu}(\mathbf{r}_i)] \rangle \quad (31)$$

is conjugate to $1/T$ and therefore, should exhibit the same singularity as the internal energy at the transition. The results obtained from the simulation are in agreement with this expectation. However, the correlation function g_{nn}^\perp appears to depend more strongly on the reduced temperature than its gauge-invariant counterpart. This makes the dependence of g_{nn} on the reduced temperature look more singular than that of the internal energy. I have not succeeded in working out an analytic explanation of this behaviour. The numerical results, however, do suggest that it may be premature to interpret the experimental results of reference [34] as evidence for the failure of the de Gennes model.

3.5 CORRELATION FUNCTIONS IN THE SUPERCONDUCTING GAUGE. — The correlation functions in the SC gauge are defined as

$$g_s(\mathbf{l}) = \frac{1}{N} \sum_i \langle \cos [\phi(\mathbf{r}_i + \mathbf{l}) - \phi(\mathbf{r}_i)] \rangle, \quad (32)$$

where the angular variables $\phi(\mathbf{r}_i)$ are related to the original variables $\theta(\mathbf{r}_i)$ by the gauge transformation defined in equations (10)-(12). As discussed in the Introduction, the critical behaviour of these correlation functions is expected to reflect the true nature of the NA transition. The numerical procedure used in the calculation of g_s is described section 2. In this calculation, I came across a problem arising from the smallness of sample size. It is evident from equation (10) that $A'_z(k_z = 0)$ is equal to zero, whereas there is no such restriction on $A'_x(\mathbf{k})$ and $A'_y(\mathbf{k})$. This asymmetry between the \parallel and \perp directions is not important in the thermodynamic limit. However, in the small samples studied in the simulation, it makes $g_s(\mathbf{l})$ anisotropic even when $K_1^0 = 0$. (For $K_1^0 = 0$, $B_0 = D_0$ and $K_2^0 = K_3^0$, the model of equation (8) reduces, *via* the gauge transformation of equations (10)-(12), to the isotropic lattice superconductor model of reference [16]. Therefore, in the thermodynamic limit where the restrictions $A'_z(k_z = 0) = 0$ are irrelevant, the correlation functions $g_s(\mathbf{l})$ should be isotropic if $K_1^0 = 0$). In order to eliminate this spurious finite-size effect, measurements of $g_s(\mathbf{l})$ were made from simulations in which the constraints given in equations (13a) and (13b) were imposed on the allowed values of the variables $A_\mu(\mathbf{r}_i)$. These constraints, which are equivalent to setting $A'_x(k_x = 0)$ and $A'_y(k_y = 0)$ equal to zero, remove the asymmetry between the \parallel and \perp directions mentioned above and restore the isotropy of $g_s(\mathbf{l})$ in the $K_1^0 = 0$ limit. For the $L = 8$ and $L = 10$ samples studied, the imposition of these constraints produces a 10-15 % increase in the value of T^* , but does not affect the critical behaviour of gauge-independent quantities in any significant way. The qualitative behaviour of short-range order-parameter correlations discussed in section 3.4 also

remains unchanged. There is, however, a significant change in the observed behaviour of the Fourier transforms of the X-ray correlation functions $g(\mathbf{l})$. The Fourier transforms $g(\mathbf{k})$ calculated from the restricted simulations closely resemble the Lorentzian form of equation (19) for both \parallel and \perp directions. Plots of $[g(\mathbf{k})]^{-1}$ versus $|\alpha_\perp(\mathbf{k})|^2$ show much less curvature. The calculated values of the ratio $\xi_\parallel^f/\xi_\perp^x$ are somewhat smaller than those obtained from the unrestricted simulations and the dependence of this ratio on the reduced temperature is weaker. These changes may be explained in the following way.

It is clear from equation (8) that the Hamiltonian of this model is invariant under the transformation

$$\begin{aligned} \theta(\mathbf{r}_i) &\rightarrow \theta(\mathbf{r}_i) + n_{ix} C_1 + n_{iy} C_2, \\ A_x(\mathbf{r}_i) &\rightarrow A_x(\mathbf{r}_i) + C_1, \\ A_y(\mathbf{r}_i) &\rightarrow A_y(\mathbf{r}_i) + C_2, \end{aligned} \quad (33)$$

where C_1 and C_2 are arbitrary constants. (Periodic boundary conditions restrict the values of C_1 and C_2 to $2\pi m/L$ where m is an integer.) In physical terms, the transformation (33) corresponds to a small global rotation of the system, which, by construction, leaves the Hamiltonian unchanged. Thus, in addition to the usual ground state, $\theta(\mathbf{r}_i) = \text{constant}$, $A_x(\mathbf{r}_i) = A_y(\mathbf{r}_i) = 0$, there are other ground states with the same energy described by $\theta(\mathbf{r}_i) = \text{constant} + n_{ix} C_1 + n_{iy} C_2$,

$$A_x(\mathbf{r}_i) = C_1, \quad A_y(\mathbf{r}_i) = C_2.$$

During a time evolution governed by the Monte Carlo dynamics described in section 2, parts of the system sometimes fluctuate into the vicinity of one of the ground states with small but non-zero values of C_1 and C_2 if the temperature is higher than T^* [41]. These fluctuations, while having no effect on the X-ray correlation function in the z -direction, do affect the correlations in the xy plane. In particular, fluctuations in the neighbourhood of a ground state with $C_1 = 2\pi m_1/L$, $C_2 = 2\pi m_2/L$ cause an enhancement of the Fourier component of $g(\mathbf{l})$ with $k_x = 2\pi m_1/L$, $k_y = 2\pi m_2/L$, $k_z = 0$. Because of this enhancement for small values of k_\perp , the observed $g(\mathbf{k}_\perp)$ appears to fall off faster than a Lorentzian for relatively large values of k_\perp . The imposition of the constraints of equation (13) suppresses these fluctuations and consequently, reduces the values of $g(\mathbf{k}_\perp)$ for small k_\perp while leaving the values of $g(\mathbf{k}_\perp)$ for large k_\perp relatively unaffected. This brings $g(\mathbf{k}_\perp)$ closer to the Lorentzian form and also causes the estimate of ξ_\perp^x to increase. Microscopic examination of the configurations generated in the Monte Carlo evolution bears out this picture.

Spontaneous fluctuating corresponding to uniform rotations of macroscopic regions of the sample are extremely unlikely to occur in real experiments.

Thus, it is possible that the non-Lorentzian behaviour of $g(\mathbf{k}_\perp)$ observed in experiments is not related to similar behaviour seen in the simulations. However, it is interesting to note that effects similar to those observed in the simulations may be produced in real systems by a different source, namely the mosaic spread of the sample. The effect of averaging over a sample in which the direction of nematic alignment is not the same everywhere would essentially be the same as that of averaging over a time evolution during which parts of the system undergo small uniform rotations. I have checked numerically (by convoluting a Lorentzian with a Gaussian mosaicity function) that a small amount of mosaic spread ($\approx 1^\circ$) would have substantial effects on the k_\perp -dependence of $g(\mathbf{k})$ at temperatures close to T_c . The resulting line shape exhibits all the qualitative features seen in the simulation and in experiments. Some of the X-ray scattering results available in the literature have been corrected [1, 26, 27] for effects of mosaicity. However, the correction procedures involve *ad hoc* assumptions (such as a Gaussian, temperature-independent mosaicity function) which may not be valid. A detailed experimental investigation of the effects of mosaicity on the X-ray scattering profile will be interesting and useful.

I found that the Fourier transforms, $g_s(\mathbf{k})$, of the SC gauge correlation functions, $g_s(\mathbf{l})$, calculated in the restricted ensemble can be fitted quite well by the Lorentzian form of equation (19), with ξ_\parallel^f and ξ_\perp^x replaced by the SC gauge correlation lengths ξ_\parallel^f and ξ_\perp^s . Results for $K_1^0 = 0.5$ and $T = 7.4$ are shown in figure 7. Values of ξ_\parallel^f and ξ_\perp^s were obtained from such fits. The inset of figure 7 shows that the observed temperature dependence of the ratio $\xi_\parallel^f/\xi_\perp^s$ as the transition is approached from the nematic side. Both ξ_\parallel^f and ξ_\perp^s change by factors of ≈ 3 (from ≈ 1.5 to ≈ 4.5) over the temperature range shown, whereas their ratio remains constant to within 5% for both values of K_1^0 . From this observation, I conclude that this phase transition is described by an isotropic fixed point. This conclusion, in turn, implies [2] that the phase transition in the de Gennes model belongs in the inverted XY universality class.

I also tested the validity of the decoupling approximation used by Lubensky and co-workers [2, 18-20] to relate the behaviour of the X-ray correlation functions to that of the correlation functions in the SC gauge. This approximation consists of two parts. For the lattice model considered here, the first part of the approximation corresponds to assuming that in the critical region in the nematic phase (and also in the entire smectic phase), the X-ray correlation function $g(\mathbf{l})$ can be factorized as

$$g(\mathbf{l}) \approx g_s(\mathbf{l}) G(\mathbf{l}) \quad (34)$$

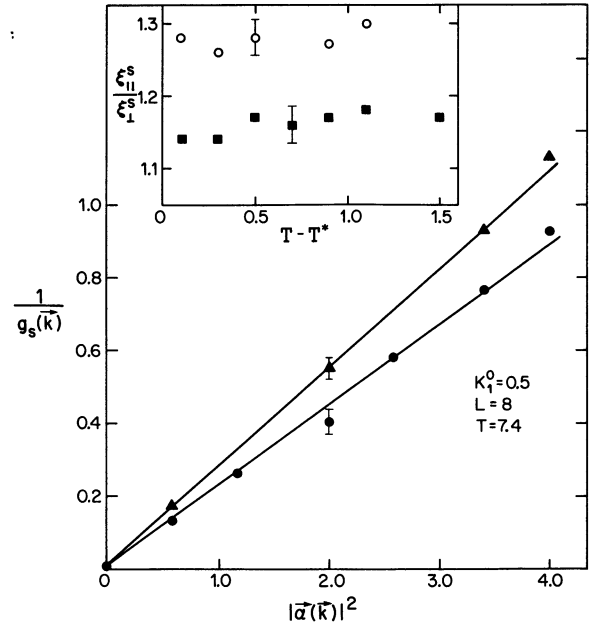


Fig. 7. — Plots of the inverse of $g_s(\mathbf{k})$, the Fourier transform of the SC gauge correlation function ($L = 8$, $K_1^0 = 0.5$, $T = 7.4$) vs. $|\alpha(\mathbf{k})|^2$ for the parallel (triangles) and perpendicular (circles) directions. The inset shows the temperature dependence of the ratio of the two SC gauge correlation lengths for $K_1^0 = 0.5$ (squares) and $K_1^0 = 5.0$ (open circles). T^* , the temperature at the specific heat peak, is 7.1 and 7.9 for $K_1^0 = 0.5$ and 5.0, respectively. The results shown here and in figures 8 and 9 were obtained from the restricted simulations described in the text.

for large values of l , where

$$G(\mathbf{l}) \equiv \frac{1}{N} \sum_{i=1}^N \langle \cos [L(\mathbf{r}_i + \mathbf{l}) - L(\mathbf{r}_i)] \rangle. \quad (35)$$

The variables $L(\mathbf{r}_i)$ appearing in equation (35) are the same as those in equations (10)-(12), which define the transformation from the LC to the SC gauge. The second part of the decoupling approximation involves the assumption that the leading large- l behaviour of $G(\mathbf{l})$ is correctly described by the lowest nonvanishing (second) cumulant. This assumption implies the following form for $G(\mathbf{l})$ in the nematic phase :

$$G(\mathbf{l}) = \exp \left[-\frac{1}{N} \sum_{\mathbf{k}} (1 - \cos(\mathbf{k} \cdot \mathbf{l})) S(\mathbf{k}) \right], \quad (36)$$

where

$$S(\mathbf{k}) = \frac{|\alpha_\perp(\mathbf{k})|^2}{[|\alpha_\perp(\mathbf{k})|^2 + |\alpha_z(\mathbf{k})|^2]^2} \times \frac{T}{K_1 |\alpha_\perp(\mathbf{k})|^2 + K_3 |\alpha_z(\mathbf{k})|^2}. \quad (37)$$

The correlation functions $G(\mathbf{l})$ were calculated directly from the simulations in the restricted en-

semble. The validity of the factorization part (Eq. (35)) of the decoupling approximation was tested by examining the l -dependence of the ratio

$$R(l) \equiv g(l)/[g_s(l)G(l)]. \quad (38)$$

The results showed consistency with equation (35) at temperatures close to T^* in the nematic phase. The observed l -dependence of $R(l)$ at $T = 7.2$ ($L = 8$, $K_1^0 = 0.5$) is shown in figure 8 for l in both \parallel and \perp directions. It appears that $R(l)$ approaches a constant value for large values of l in either direction. The asymptotic value of $R(l)$ was found to depend weakly on the direction of l and on the temperature. The validity of the second part (Eqs. (36) and (37))

of the decoupling approximation was examined by calculating the quantities

$$U(\mathbf{k}) = - \sum_l \ln [G(l)] e^{i\mathbf{k}\cdot\mathbf{l}}, \quad (39)$$

which, according to equation (36), should be equal to $S(\mathbf{k})$ given in equation (37). The data were found to be consistent with this expectation. The results for $U(\mathbf{k})$ at $T = 7.2$ ($L = 8$, $K_1^0 = 0.5$) are shown in figure 9. The solid lines, which represent the \mathbf{k} -dependence expected from equation (37) with $K_1 = 0.5$ and $K_3 = 1.25$, clearly provide a good description of the data. Thus, the observed gauge-dependence of the correlation functions appears to be well-described by the decoupling approximation for T close to T^* in the nematic phase. I also found good agreement with the decoupling approximation at all temperatures lower than T^* .

4. Concluding remarks.

To summarize, two main conclusions may be derived from the present work. First, the fact that several features observed in experiments are qualitatively reproduced in the simulation provides strong support to the validity of the de Gennes model. Second, calculations of correlation functions in the SC gauge indicate that (a) the phase transition in the de Gennes model belongs in the inverted XY universality class for small as well as large values of the splay elastic constant, and (b) the gauge-dependence of the correlation functions is well-described by the decoupling approximation in the critical region. These results imply that in the NA transition, all gauge-invariant quantities should exhibit inverted XY behaviour, and the X-ray correlation lengths should show a crossover from isotropic to anisotropic critical behaviour as the transition is approached from the nematic side.

The fact that some of the experimental results do not agree with these predictions remains somewhat puzzling. The apparent non-universality of the critical behaviour observed in experiments suggests the presence of crossover effects. One source of crossover effects (namely, the presence of a nearby tricritical point) in materials with narrow nematic ranges has already been identified. Other crossover phenomena (mean-field to critical, regular XY to inverted XY) and correction-to-scaling effects arising from the presence of a large splay elastic term may be important in understanding the experimentally observed critical behaviour in some systems. Quantitative calculations of these effects would be very useful in clarifying the situation. On the experimental side, the true nature of the NA transition is most likely to be observed in materials with a broad nematic range and small values of the splay elastic constant and the layer spacing. Efforts toward

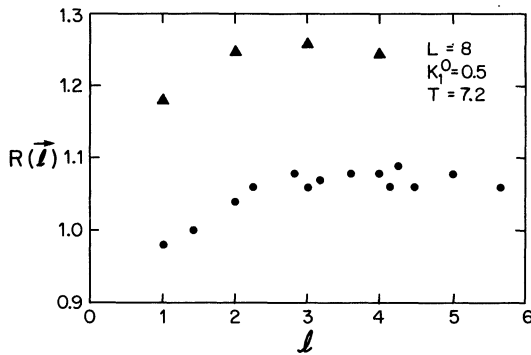


Fig. 8. — The ratio $R(l)$ defined in equation (38) vs. l for $L = 8$, $K_1^0 = 0.5$, $T = 7.2$, and l in the parallel (triangles) and perpendicular (circles) directions.

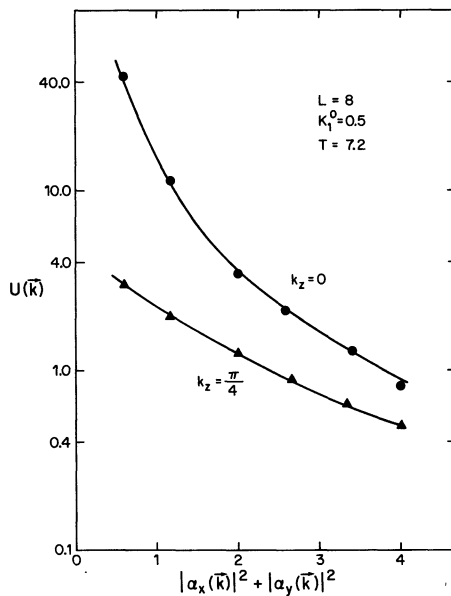


Fig. 9. — Plots of the quantity $U(\mathbf{k})$ defined in equation (39) vs. $[|\alpha_x(\mathbf{k})|^2 + |\alpha_y(\mathbf{k})|^2]$ for $L = 8$, $K_1^0 = 0.5$, $T = 7.2$, and two different values of k_z (circles : $k_z = 0$; triangles : $k_z = \pi/4$). The solid lines represent the behaviour expected from equation (37) with $K_1 = 0.5$ and $K_3 = 1.25$.

synthesizing materials with these properties would be most welcome. A careful experimental study of the effects of mosaicity on the X-ray scattering profile may provide important insight into the puzzling behaviour of the X-ray correlation lengths.

5. Acknowledgments.

This study was initiated during a visit to the Physics

Department of Harvard University. I am grateful to B. I. Halperin for his hospitality and many helpful discussions. I have also benefitted from discussions with C. C. Huang, T. C. Lubensky and J. Toner. This work was supported by a Research Fellowship awarded by the Alfred P. Sloan Foundation, and by a grant for CRAY time from the Minnesota Supercomputer Institute.

References

- [1] For a review of experimental work, see LITSTER, J. D., BIRGENEAU, R. J., KAPLAN, M., SAFINYA, C. R. and ALS-NIELSEN, J. in *Ordering in Strongly Fluctuating Condensed Matter Systems*, edited by T. Riste (Plenum, New York 1980, p. 357).
- [2] For a review of theoretical work, see T. C. Lubensky, *J. Chim. Phys.* **80** (1983) 31.
- [3] P. G. DE GENNES, *Solid State Commun.* **10** (1972) 753 ; *Mol. Cryst. Liq. Cryst.* **21** (1973) 41.
- [4] The de Gennes model omits certain higher order potentials (see GRINSTEIN, G. and PELCOVITS, R. A., *Phys. Rev. Lett.* **47** (1981) 1202) which ensure global rotational invariance for large angles of rotation. It is believed that these potentials, although important deep in the smectic-A phase, do not affect the critical properties at the NA transition.
- [5] HALPERIN, B. I., LUBENSKY, T. C. and MA, S.-K., *Phys. Rev. Lett.* **32** (1974) 292.
- [6] HALPERIN, B. I. and LUBENSKY, T. C., *Solid State Commun.* **14** (1976) 997.
- [7] LUBENSKY, T. C. and CHEN, J.-H., *Phys. Rev. B* **17** (1978) 366.
- [8] LANDAU, L. D. and LIFSHITZ, E. M. in *Statistical Physics* (Addison-Wesley, Reading, Mass.) 1969, p. 402.
- [9] CAILLÉ, A., *C. R. Heb. Séan. Acad. Sci.* **B 274** (1972) 891.
- [10] FRANK, F. C., *Disc. Faraday Soc.* **29** (1958) 1.
- [11] HELFRICH, W., *J. Physique* **39** (1978) 1199.
- [12] NELSON, D. R. and TONER, J., *Phys. Rev. B* **24** (1981) 363.
- [13] TONER, J., *Phys. Rev. B* **26** (1982) 462.
- [14] DASGUPTA, C., *Phys. Rev. A* **27** (1983) 1262.
- [15] DAY, A. R., LUBENSKY, T. C. and MCKANE, A. J., *Phys. Rev. A* **27** (1983) 1461.
- [16] DASGUPTA, C. and HALPERIN, B. I., *Phys. Rev. Lett.* **47** (1981) 1556.
- [17] BARTHOLOMEW, J., *Phys. Rev. B* **28** (1983) 5378.
- [18] LUBENSKY, T. C., DUNN, S. G. and ISAACSON, J., *Phys. Rev. Lett.* **47** (1981) 1609.
- [19] LUBENSKY, T. C. and MCKANE, A. J., *Phys. Rev. A* **29** (1984) 317.
- [20] DUNN, S. G. and LUBENSKY, T. C., *J. Physique* **42** (1981) 1201.
- [21] LE GUILLOU, J. C. and ZINN-JUSTIN, J., *Phys. Rev. Lett.* **47** (1981) 43.
- [22] THOEN, J., MARYNISSEN, H. and VAN DAEL, W., *Phys. Rev. Lett.* **52** (1984) 204.
- [23] OCKO, B. M., BIRGENEAU, R. J., LITSTER, J. D. and NEUBERT, M. E., *Phys. Rev. Lett.* **52** (1984) 208.
- [24] GARLAND, C. W., MEICHLER, M., OCKO, B. M., KORTAN, A. R., SAFINYA, C. R., YU, L. J., LITSTER, J. D. and BIRGENEAU, R. J., *Phys. Rev. A* **27** (1983) 3234.
- [25] SCHNATZ, C. A. and JOHNSON, D. L., *Phys. Rev. A* **17** (1978) 1504.
- [26] LITSTER, J. D., BIRGENEAU, R. J., AL-NIELSEN, J., DAVIDOV, D., DANA, S. S., GARCIA-GOLDING, F., KAPLAN, M., SAFINYA, C. R. and SCAETZING, R., *J. Physique Colloq.* **40** (1979) C3-339.
- [27] DAVIDOV, D., SAFINYA, C. R., KAPLAN, M., DANA, S. S., SCAETZING, R., BIRGENEAU, R. J. and LITSTER, J. D., *Phys. Rev. B* **19** (1979) 1657.
- [28] SPRUNT, S., SOLOMON, L. and LITSTER, J. D., *Phys. Rev. Lett.* **53** (1984) 1923.
- [29] MAHMOOD, R., BRISBIN, D., KHAN, I., GOODEN, C., BALDWIN, A., JOHNSON, D. L. and NEUBERT, M. E., *Phys. Rev. Lett.* **54** (1985) 1031.
- [30] GOODEN, C., MAHMOOD, R., BRISBIN, D., BALDWIN, A., JOHNSON, D. L. and NEUBERT, M. E., *Phys. Rev. Lett.* **54** (1985) 1035.
- [31] BIRECKI, H., SCAETZING, R., RONDELEZ, F. and LITSTER, J. D., *Phys. Rev. Lett.* **36** (1976) 1376.
- [32] VON KANEL, H. and LITSTER, J. D., *Phys. Rev. B* **23** (1981) 3251.
- [33] FISCH, M. R., SORENSEN, L. B. and PERSHAN, P. S., *Phys. Rev. Lett.* **47** (1984) 43.
- [34] CHAN, K. K., DEUTSCH, M., OCKO, B. M., PERSHAN, P. S. and SORENSEN, L. B., *Phys. Rev. Lett.* **54** (1985) 920.
- [35] DASGUPTA, C., *Phys. Rev. Lett.* **55** (1985) 1771.
- [36] See, e.g. *Monte Carlo Methods in Statistical Physics*, edited by K. Binder (Springer, Berlin) 1979.
- [37] BARMATZ, M., HOHENBERG, P. C. and KORNBLIT, A., *Phys. Rev. B* **12** (1975) 1947.
- [38] See e.g. BARBAR, M. N. in *Phase Transitions and Critical Phenomena* **8**, edited by C. Domb and J. Lebowitz (Academic, New York) 1983.
- [39] ALS-NIELSEN, J., BIRGENEAU, R. J., KAPLAN, M., LITSTER, J. D. and SAFINYA, C. R., *Phys. Rev. Lett.* **39** (1977) 352 ; *Phys. Rev. Lett. (E)* **41** (1978) 1626.
- [40] JÄHNIG, F. and BROCHARD, F., *J. Physique* **35** (1974) 301.
- [41] In a few Monte Carlo runs, the system condensed upon cooling into an ordered state with non-zero values of C_1 and/or C_2 . These runs were excluded from the calculation of averages.